Heritage Science

RESEARCH

Open Access

Mechanical properties and moisture-related dimensional change of canvas paintings–canvas and glue sizing

Arkadiusz Janas[1], Laura Fuster-López[2], Cecil Krarup Andersen[3], Angel Vicente Escuder[4], Roman Kozłowski[1], Katarzyna Poznańska[1], Aleksandra Gajda[1], Mikkel Scharff[3] and Łukasz Bratasz[1*]

Abstract

Understanding canvas paintings as physical systems is fundamental to develop evidence-based environmental specifications for museums. A number of tests were carried out to determine mechanical properties of canvas, canvas sized with animal glue and animal glue-based ground layer (gesso) as a function of relative humidity (RH). The mechanical properties of the canvas samples tested exhibited an anisotropy dependent on the measurement direction, being the stiffness corresponding to the weft direction greater than the warp and diagonal ones. Sizing the canvas with a layer of animal glue significantly increased its modulus of elasticity while the anisotropy of mechanical properties was kept in the composite material. The application of an animal glue-based ground layer on sized canvas increased the elasticity modulus of the system by another order of magnitude (~ 2 GPa) whereas the anisotropy of the material disappeared. The measurements were carried out in a wide range of RH from 30 to 90%. An increase in RH caused a decrease in the material stiffness. Cracking of the gesso layer, which is often responsible for the formation of cracks in paintings, was observed at strains of the order of a few thousandths. Swelling of glue sizing dominated the moisture-induced swelling of the composite material in the less stiff warp direction, completely overriding the shrinkage of the untreated canvas. In contrast, the swelling of the composite material in the stiffer weft direction was much smaller than for pure glue alone, being clearly affected by the textile.

Keywords: Canvas paintings, Canvas, Sized canvas, Gesso layer, Animal glue, Tensile properties, Dimensional change

Introduction

Paintings on canvas are complex multi-layered structures composed of humidity-sensitive materials: canvas support sized with animal glue, a ground preparatory layer, and paint and varnish layers on the top. Further, paintings may also comprise materials added in conservation treatments to reinforce or stabilize the painted structure. The materials respond to changes in relative humidity (RH)—they shrink when they lose moisture and swell when they gain moisture. Owing to different moisture expansion coefficients of materials together with other specific characteristics such as woven geometry in canvases, each material responds differently to this loss and gain of moisture [1]. The mismatch may generate stresses in the layered structure leading to deformation, cracking, and delamination. Further, shrinkage of the fresh pictorial layer during drying and film forming processes needs to be taken into account to fully describe the mechanics of paintings [2, 3]. The initial shrinkage engendered in the glue and glue-based grounds during drying is followed by further cumulative shrinkage, when the materials are subjected to subsequent cycles of exposure to high RH levels, owing to the recovery of strains formed during the initial drying.

*Correspondence: lukasz.bratasz@ikifp.edu.pl

[1] Jerzy Haber Institute of Catalysis and Surface Chemistry Polish Academy of Sciences, 30-239 Kraków, Poland
Full list of author information is available at the end of the article

Canvas paintings are thus among the types of complex cultural objects which are considered to be vulnerable to climate-induced degradation and damage. As canvas paintings are predominant in collections worldwide, tight environmental controls are generally set in museums as a way to reduce the possibility of degradation, which involves energy-intensive air conditioning systems. Scientific understanding of how changes in environmental conditions affect canvas paintings is therefore a pathway to the development of more sustainable and evidence-based guidelines for climate regulation strategies in museums and historic buildings.

In 1982, Mecklenburg proposed a laminar structural model of canvas paintings [4] which was further developed based on studies of the moisture-related dimensional response and tensile properties of individual layers of the paintings: the support canvas, a glue size layer, oil or glue-based ground and paints in the design layer [1]. The model was based on the principle of superposition and assumed that the overall structural response of a painting was obtained by superimposing individual responses of all components together. The model has identified two humidity conditions at which high forces are developed in the assembly of the layers that constitute the painting when it is restrained and subjected to change in RH. One is at the very high levels of RH, usually above 80%, at which a dramatic shrinkage can be observed in the linen canvas, generally in the warp direction [1, 4–6]. When restrained, the shrinkage shows up as significant stress in the textile. The other is at the very low RH levels as the glue size experiences shrinkage with decreasing RH and develops high stress when restrained. In contrast to the canvas, glue loses all stiffness and strength at high RH levels, which is triggered by a transition from a brittle to ductile state. In general, forces developed in restrained and desiccated oil paints and ground are considerably less than in the canvas and the glue size, also because the ground contains a large volume fraction of non-adsorbing filler and, frequently, oil as a binder. The model predictions agreed well with the measured force development in actual paintings and allowed the damage mechanism to be accounted for, especially tenting and flaking of the pictorial layer on shrinkage of the canvas if loose, or mechanical damage of a degraded canvas. However, the laminar model could not explain the moisture sensitivity of canvas paintings lined with wax-resin adhesive, unless canvas and adhesive were perceived as one layer [7, 8].

The structural information on canvas paintings has been enriched by visualisation and quantification of the spatial distribution of moisture in painting samples at the resolution of a few tens of micrometres with the use of neutron radiography [9]. On steps in RH from dry to 90%, collagen glue absorbed a high amount of moisture per weight and a local moisture surplus was used to map the distribution of glue in the structure. The glue content in the canvas was higher when the size was applied in a form of a liquid easily penetrating into the canvas compared to the gel-sized canvas. In contrast, a gel size penetrated less and stayed close to the canvas surface. The observation was confirmed by measurements of the resistance of the layers to water vapour flow [10]. The study focused on a specific layered build-up composed of linen canvas, glue sizing, chalk-glue ground and oil paint with umber pigment typical of the Swiss painter Cuno Amiet (1868–1961) and, more broadly, of the international art scene of that period. The measurements demonstrated that the method of applying glue sizing on a canvas influenced the permeability of the resulting sized canvas. The dispersed glue in the case of the liquid size led to lower vapour resistance as opposed to the more localized and film-forming gel size which was representing a more discrete layer in the laminate. The lower the temperature of the sizing glue during the application, the higher its viscosity, the more it formed a film and the more it hindered vapour transmission. The addition of the ground layer led to a further increase in the vapour resistance and finally the oil paint, despite its limited thickness relative to the other layers, showed by far the largest inhibiting effect on the vapour flow.

The structural features of canvas paintings discussed above indicate that information on moisture-related dimensional response and tensile properties of individual layers might not capture the full complexity of the system. In consequence, additional information quantifying the properties of layered structured consecutively produced in the process of painting execution, starting from the canvas, through the glue-sized canvas, to the glue-sized canvas coated with a ground layer needs to be obtained. It was previously shown by multiple authors that a canvas has orthotropic properties depending on the weave directions [11–13]. These different properties are reflected in the mechanical and structural responses of lined or impregnated canvas paintings [7, 8]. Using the uniaxial extension, it has been demonstrated that the strong anisotropy of the support canvas (mechanical properties of painting canvas under tensile loading at varying angles in relation to the selected direction) decreases with an increasing number of glue-chalk ground layers applied on the glues-sized canvas, while the isotropic character of the system becomes predominant [14]. The aim of the present study has been to obtain systematic information on the layered structure analysed. The chosen materials included several types of linen canvas and animal glue sizing, as well as different methods of glue size application. The chalk-glue ground was selected to represent generally a 'design layer' in historic canvas

paintings. On the one hand, though oil grounds predominate in canvas paintings, chalk-glue grounds were popular among painters throughout European art history and are described in many historical recipes, also as a first layer followed by a second oil-bound layer [10, 15]. On the other hand, the mechanical properties of oil-based pictorial layers are known to evolve up to 150 years after painting [16]. Therefore, mock-up paintings with young oil-based layers naturally aged for a limited time would not mimic old historic paintings in terms of their structural behaviour. In consequence, the chalk-glue ground layers having mechanical properties close to old brittle oil-based materials can be used as substitutes for the historic design layers [1, 17].

Materials and methods

Two close weave and one open weave linen canvases were used (Table 1, Fig. 1). All the canvases were washed in pure warm water (30 °C). The thicknesses of untreated canvases were assessed microscopically. Canvases are not homogenous materials but woven structures constructed of interlocked fibres – yarns. Canvases are comparatively stiff in the direction of the yarns but flexible on bending. To numerically model the canvas, Mecklenburg and Tumosa measured a mean fibre cross-section area per yarn in the separated warp and weft yarns obtained from three different canvases [18]. The authors found that the parameter was on average only 0.22 of the nominal textile area per yarn, calculated from the measured canvas thickness. The effective thickness of 'compact' fibre layer in the canvases analysed in this work was accordingly calculated from the measured textile thickness and number of yarns on the assumption of 0.22 as the ratio between the fibre and nominal cross-section areas per yarn, respectively (Table 1).

Three sets of specimens were prepared using two types of glue (Table 2). The glue size, obtained by hydrating and dissolving the glue in water at 60 °C, was applied to the canvas stretched on the wooden frame. Gel (cold) and liquid (warm) consistencies of the glues were tested, the glue concentrations for each application are given in Table 2. The glue solution was applied with a brush when still warm (ca. 45 °C), or with a knife when the glue was cold and in form of gel (ca. 20 °C). One glue-sized canvas was further covered with a glue-chalk ground layer of the pigment volume concentration (PVC) of 92% and 1:14 glue water ratio. $PVC = P/(P + B)$ where P and B are volumes of the pigment and the dried glue binder, respectively and the ratio is expressed in per cent. Chalk from Bologna (ref. 58100) from Kremer Pigments was used. To

Table 1 Details of linen canvases

Name	No threads in the weft x warp weave directions (/cm)	Cover factor (%)	Thickness (mm)	Effective thickness of the fibre layer (mm)		Weave
				Weft	Warp	
PL	16 × 16	98.5	0.47	0.10	0.10	Close
CTS 1111	13 × 15	96	0.64	0.12	0.14	Close
CTS 2297	9 × 9	74	0.49	0.08	0.08	Open

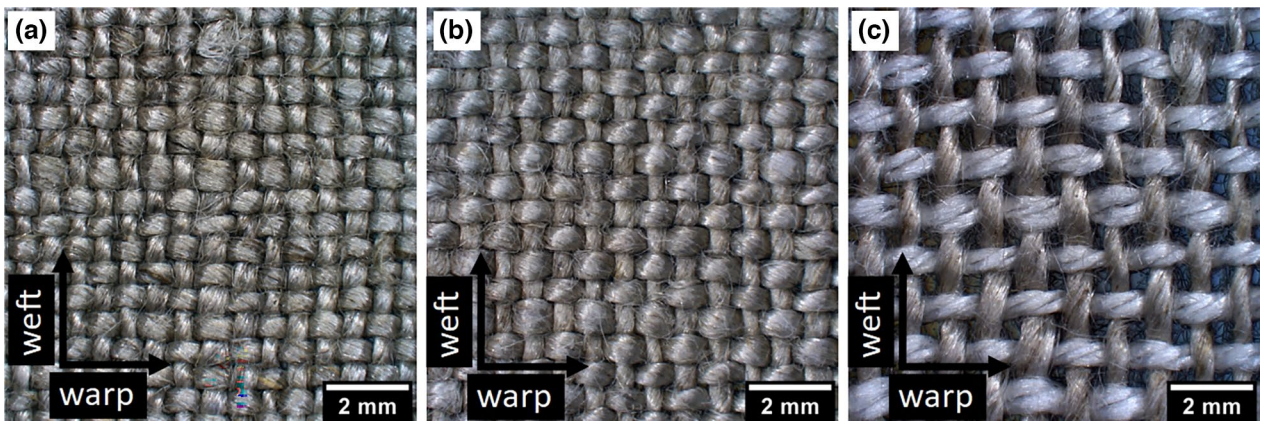

Fig. 1 Microscopic images of the canvases: **a** PL close weave canvas; **b** CTS close weave canvas; **c** CTS open weave canvas. The warp and weft directions are indicated

Table 2 Details of specimens prepared in various ways, investigated in the study

Sizing		Name	Amount of glue (kg/m^2)	Thickness (mm)	Effective thickness of the fiber-glue layer (mm)		Description
					Weft	Warp	
Rabbit skin glue Kremer ref. 63028	Gel	PL canvas 63028 gel-sized	0.018	0.48	0.116	0.116	Canvas sized with glue gel (5% w/w) applied with a knife in the cold state. Two glue layers
	Liquid	PL canvas 63028 liquid-sized	0.025	0.52	0.121	0.121	Canvas sized with glue aqueous solution (15% w/w) applied with a brush in the warm state. Single glue layer
	Gel	PL canvas 63028 gel-sized + ground layer	–	0.75	–	–	Canvas sized with glue gel as described above with a further chalk-glue ground layer (92% PVC)
Rabbit skin glue Kremer ref. 63028	Gel	CTS 1111 canvas 63028 gel-sized	0.076	0.69	0.179	0.199	Canvas sized with glue gel (10% w/w) applied with a knife in the cold state
		CTS 2297 canvas 63028 gel-sized	0.078	0.67	0.141	0.141	
	Liquid	CTS 1111 canvas 63028 liquid-sized	0.041	0.72	0.152	0.172	Canvas sized with glue aqueous solution (10% w/w) applied with a brush in the warm state
		CTS 2297 canvas 63028 liquid-sized	0.036	0.61	0.112	0.112	
Bone glue Kremer ref. 63000	Gel	CTS 1111 canvas 63000 gel-sized	0.055	0.73	0.163	0.183	Canvas sized with glue gel (10% w/w) applied with a knife in the cold state
		CTS 2297 canvas 63000 gel-sized	0.130	0.62	0.182	0.182	
	Liquid	CTS 1111 canvas 63000 liquid-sized	0.066	0.77	0.171	0.191	Canvas sized with glue aqueous solution (10% w/w) applied with a brush in the warm state
		CTS 2297 canvas 63000 liquid-sized	0.033	0.64	0.106	0.106	

prepare the ground, chalk was slowly added to the warm glue solution until no liquid was visible. The thicknesses of all treated canvases were measured with a micrometric screw after the specimens had dried at room conditions. The effective thickness of 'compact' fibre-glue layer in the glue-sized canvases was calculated by adding the effective thicknesses of the fibre layer, listed in Table 1, and the glue size layer, the latter calculated from the amount of glue and its density of 1.27 g/cm^3 (Table 2).

The tensile properties were determined using a Universal Testing Machine (UTM) from Hegewald & Peschke MPT GMBH (Nossen, Germany) for specimens 80–100 mm long and 25–50 mm wide. The specimen was mounted loosely before the loading started. The rate of tension loading was 1 mm/min. Each specimen investigated was placed in a sealed box connected to a climatic chamber which allowed RH to be precisely controlled. All measurements were taken at laboratory temperature ranging between 22 and 24 °C and at four selected RH levels of 30, 50, 75 and 90%. To ensure that moisture content in the material reached the new equilibrium on each RH shift, cycles of loading the specimen up to 0.2 kN/m were repeated at 10 min intervals. After each cycle, the initial position of the specimen was reached. The specimen was considered to have reached 'equilibrium' when the slope of the subsequent load-extension curves was constant. The time of specimen equilibration never exceeded 1 h. The measurements described were done in two perpendicular weave directions of the substrate canvas, weft and warp, as well as along the bias direction (at an angle of 45° to warp/weft).

Additionally, the dimensional change accompanying water vapour adsorption and desorption was measured in the warp and weft directions for a selected set of samples – CTS 1111 and 2297 canvases sized with bone glue (ref. 63000) applied with a brush in the warm state. Strip specimens 25 mm × 100 mm were used. The specimen was mounted in UTM. The machine was programmed to keep it unloaded until the equilibration at a set RH value. The time of equilibration was 2 and 3 h in the RH ranges of 30–60% and 70–95%, respectively. Then the specimen was loaded with stress of 0.06 kN/m to keep it in a vertical plane and the dimensional change was recorded. Four pairs of reference points were applied with the black marker evenly across the specimen width, typically at a distance of 4 mm from the UTM jaws. Dimensional change was recorded using optical extensometer ONE from the same manufacturer as UTM. The strain was calculated as an average of four measurements unless recorded values were corrupted due to loss of reference point recognition. Both expansion and shrinkage branches of the dimensional change isotherm were

recorded, starting at the initial RH of 50% which is the midpoint of the full RH scale between 0 and 100%.

Additionally, Poisson's ratio was determined for warp and weft directions for the same samples. Due to out-of-plane deformation of specimens disturbing strain measurements in the direction transversal to the load, the Poisson's ratio was determined at the load of 0.3 kN/m. The optical extensometer was used again to measure the specimen deformation in a direction along the load application and across, using four pairs of points in each direction. The measurement for each specimen was repeated between 9–13 times, that is to say after each consecutive measurement the specimen was removed from UTM, remounted and a new measurement was carried out.

Results and discussion

Tensile properties

Load-extension curves in the three weave directions obtained for the PL canvas at 50% RH illustrate subsequent phases of the textile deformation by increasing load (Fig. 2). Strain is expressed as the change in length divided by the specimen's original length and load is expressed as the force per width of a specimen.

It is generally accepted that the initial part of the load-extension curve corresponds to a slack region before the tension is taken up by the textile, followed by a crimp-removal region. Only the post-initial relationship reflects the stretching of the yarns (the Hookean region). The plots indicate a transition to the Hookean region above an extension of at least 5%, which manifests as a gradual increase in stiffness. The load-extension relationships become finally linear until the load-extension curve begins to deviate significantly from a straight line, defining the upper limit of the elastic range at which non-recoverable deformation begins. The final part of the curve shows a progressive drop in load values corresponding to a successive yarn fracture. Due to the manufacturing method, the three weave directions investigated show different load-extension behaviour. The warp direction is more flexible than the weft which is attributed to a higher crimp in this direction. The bias direction is the most flexible of the three analysed. The initial load-extension range is most relevant for the analysis of canvas paintings as the application of a biaxial tension in the range 0.12–0.24 kN/m to cruciform specimens was reported to produce a tautness equivalent to that of a newly stretched painting [13]. Another study stated that classical easel paintings had tensions of around 0.2 kN/m marked in Fig. 2 with a black dashed line [19].

Glue sizing led to a considerable increase in stiffness of the canvas caused by penetration of the glue (Fig. 3). The sizing changed radically the initial part of the load-extension curve, reflecting a transition from textile with characteristic slack- and crimp-removal regions to a canvas-glue composite of high stiffness controlled by the glue even at low loading. A comparison of the load-extensions curves in the perpendicular weft and warp directions demonstrates anisotropy in the sized canvas response to loading. The observed strong anisotropy indicates that sizing transforms yarns into a glue-textile composite rather than a laminate with a thin glue film bridging uniformly the gaps in the weave of the canvas. The equivalent thickness of such hypothetical glue film would range between 15 and 100 µm (Table 2). Owing to the high modulus of elasticity of animal glues, the estimated difference between the effective moduli of elasticity in the warp and weft directions of the laminate consisting of discrete layers of glue and canvas would be on average only 13% and maximally 30%.

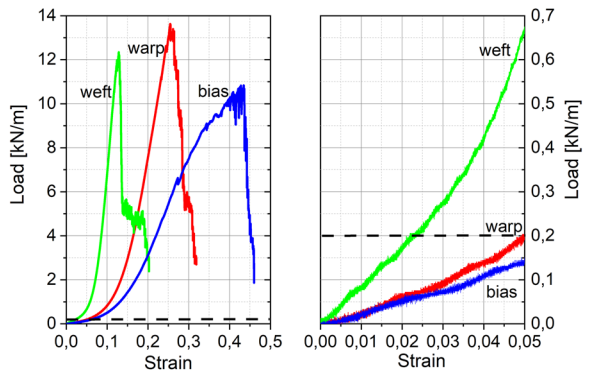

Fig. 2 Load-extension curves for untreated PL canvas subjected to tension at 50% RH. Load value of 0.2 kN/m is accepted as experienced by a well-tensioned canvas painting on its stretcher and is marked with a black dashed line

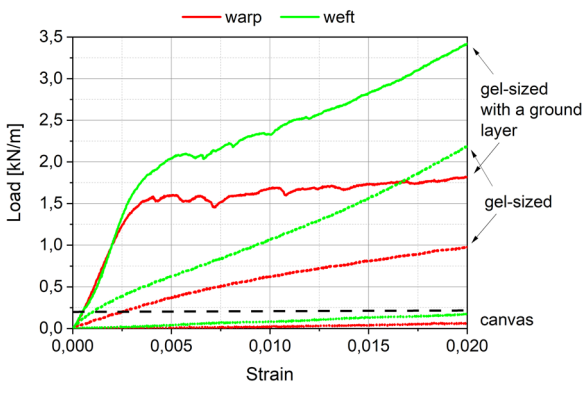

Fig. 3 Load-extension curves for PL canvas—untreated, gel-sized, gel-sized and coated with a layer of ground—subjected to tension at 50% RH. The load value of 0.2 kN/m experienced by a well-tensioned canvas painting is marked with a black dashed line

When a glue-sized canvas is further covered with a glue-chalk ground layer, the isotropic character of the system formed becomes predominant as no difference in the load-extensions curves is observed between the different weave directions for the strain range between 0 and 0.002 (Fig. 3). The critical strain of approximately 0.002 corresponds to the elongation at break for stiff and brittle glue-based grounds at the RH low- and mid-ranges determined in many laboratory studies [1, 2, 20]. With strain increasing beyond the 0.002 threshold, the ground layer fractures and the tension is taken up by the sized textile alone with differences in the load-extensions relationships reflecting the weave structure.

The initial parts of load-extension curves, corresponding generally to a slack-removal region, are linear in the load range 0–0.2 kN/m identified as the most relevant in the analysis of canvas paintings. Therefore, the nominal moduli of elasticity, representing approximately the initial stiffness, were calculated at 0.2 kN/m for all RH levels and specimens investigated using the measured thicknesses of the specimens (Tables 1 and 2). For numerical modelling purposes, the effective fibre or fibre-glue moduli of elasticity can be calculated using the effective thicknesses of fibre or fibre-glue layers provided in the same tables. To establish uncertainty in the measurements and variability among specimens collected from the same material, the load-extension curves were recorded at 50% RH in the warp direction for four specimens collected from various spots on the 63000 liquid-sized CTS 1111 canvas. The measurement for each specimen was repeated five times, that is to say after each consecutive measurement the specimen was removed from UTM, remounted and a new measurement was carried out. The average values of the nominal moduli of elasticity determined and the standard deviations of the data are shown in Fig. 4.

Whilst uncertainty in the measurements of modulus of elasticity was low, the variability among the specimens collected from various spots of the material was higher – specimen 3 exhibited a significantly lower value than the remaining three specimens. The reason for the increased variability laid in the inhomogeneity of glue distribution over the canvas surface. Digital microscopy was used to scan the surface of specimens 1 and 3 with micrometric resolution to determine the structure of the impregnated canvas. Stiffer specimen 1 showed a uniform impregnation of the yarns with the glue generally bridging the gaps in the weave of the canvas (Fig. 5). In contrast, specimen 3 exhibited less glue in the canvas structure with no glue in many gaps in the weave. The demonstrated inhomogeneity, undoubtedly due to the manual application of the glue, needs to be considered as an inherent characteristic of the material.

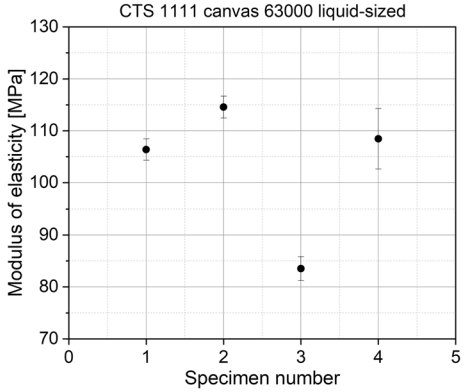

Fig. 4 Average nominal moduli of elasticity—in the warp direction—of four specimens sampled from various spots on the CTS 1111 canvas liquid-sized with glue 63000

The nominal moduli of elasticity measured at a given RH and weave direction for specimens sampled from a range of materials listed in Table 2 did not correlate reliably with the woven geometries of canvases, the types of glue and the application procedures. They are listed in an Additional file 1 and Table 3 gives their average values for each RH level and weave direction with standard deviations to illustrate the specimen-to-specimen variability.

All glue-sized specimens experience a dramatic loss of stiffness at the high RH range (Fig. 6). The material's glass transition, that is to say from the brittle to ductile (gel-like) state, is observed, a tendency well documented in earlier studies [1, 19, 21]. The relationship between the nominal moduli of elasticity of the glue-sized canvases and RH is described in this study by the four-parameter Boltzmann sigmoid function:

$$E(RH, T = const.) = \frac{A_1 - A_2}{\left(1 + e^{(RH - RH_0)/dRH}\right)} + A_2 \quad (1)$$

where E is the nominal modulus of elasticity in the given weave direction in MPa, RH—relative humidity in per cent, A_1 and A_2—the initial and final values of E, RH_0—the RH level at which E diminishes by a half difference between A_1 and A_2, corresponding to the transition of glue from the glassy to rubbery state, and dRH—the rate of the decrease in E.

First, RH_0 was established to be 78.5% at the temperatures between 22 and 24 °C from the viscoelastic data for rabbit skin glue measured by Bridarolli et al. [21]. It was also found from the same data that dRH does not change with temperature and is approximately 3.5. Finally, the A_1 and A_2 parameters were obtained by fitting to Eq. 1 the entire sets of E values determined for three weave directions in the broad group of the materials analysed. As the

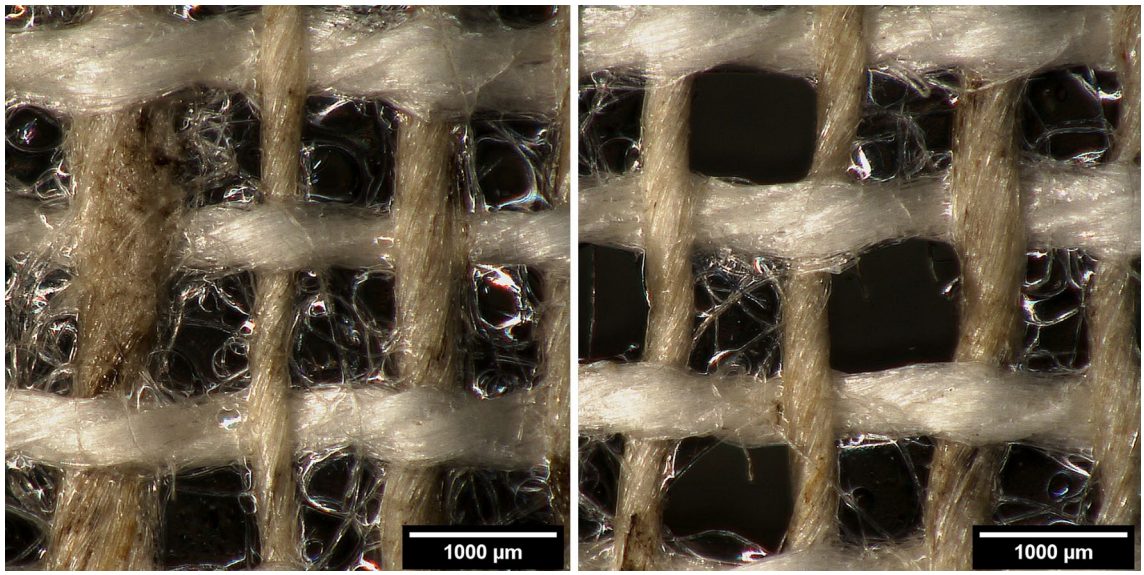

Fig. 5 Digital micrographs of specimens 1 (left) and 3 (right) sampled from the CTS 1111 canvas liquid-sized with glue 63000. The moduli of elasticity for the specimens are shown in Fig. 4

Table 3 Average nominal moduli of elasticity *E* determined for varying RH levels in three weave directions for the entire set of glue-sized canvases analysed

Weave direction	Average $E \pm$ std. dev			
	30% RH	50% RH	75% RH	90% RH
weft	470 ± 160	550 ± 240	430 ± 220	120 ± 20
warp	200 ± 120	160 ± 86	110 ± 64	30 ± 19
bias	180 ± 64	180 ± 80	110 ± 77	13 ± 22

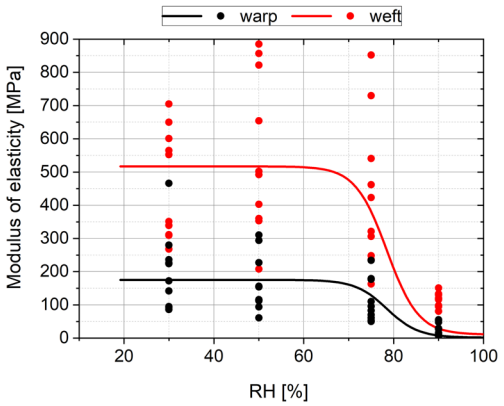

Fig. 6 Nominal moduli of elasticity for the entire set of glue-sized canvases analysed versus RH are compared with the average curves calculated for the warp and weft directions from the least-square regression of the data to the Boltzmann sigmoid function; for the sake of clarity the averaged curve for the bias direction was not included due to significant overlap with the curve for the warp direction

change of material properties of sized canvases above 78% RH results from the glassy-rubbery phase change in the glue, not in the canvas, the estimates of RH_0 and dRH were fixed in the fitting procedure. The parameters and R-square values for each direction are given in Table 4.

The Poisson's ratios ν determined in the study are given in Table 5.

Dimensional change isotherms

The dimensional response of the CTS 1111 canvas liquid-sized with glue 63000 in the warp direction subjected to three RH cycles between the dry condition and 95% RH is shown in Fig. 7. A restricted response, especially in the shrinkage range between 50 and 30% RH is observed in the first shrinkage–expansion cycle whilst the fully pronounced and reversible response is observed in the two subsequent cycles. As the glue size had been applied to the canvas stretched on the wooden frame, clearly, the specimen was to some extent elongated at the onset of the first cycle and a structural reconfiguration at high RH followed by unrestrained shrinkage to low RH was necessary to achieve the full repeatable response.

Moisture-related dimensional changes in the warp and weft directions, recorded in the third RH cycle for the canvases CTS 1111 and CTS 2297 liquid-sized with glue 63000 are compared with the same data for the canvases alone in Fig. 8. The untreated close weave

Table 4 Parameters in the Boltzmann sigmoid function obtained from the regression of the sets of *E* values determined for three weave directions for the entire set of the glue-sized canvases analysed

Weave direction	Boltzmann function parameters for groups of specimens				
	A_1 (MPa)	A_2 (MPa)	RH_0 (%)	*dRH*	R-squared
weft	517	107	78.5	3.5	0.44
warp	175	15	78.5	3.5	0.39
bias	173	3	78.5	3.5	0.54

Table 5 Poisson's ratio *v* determined for canvases CTS 1111 and CTS 2297 sized with bone glue applied in the warm state

Direction of load application	Average v ± std. dev	
	CTS 1111	CTS 2297
weft	0.62 ± 0.15	0.57 ± 0.15
warp	0.26 ± 0.06	0.25 ± 0.04

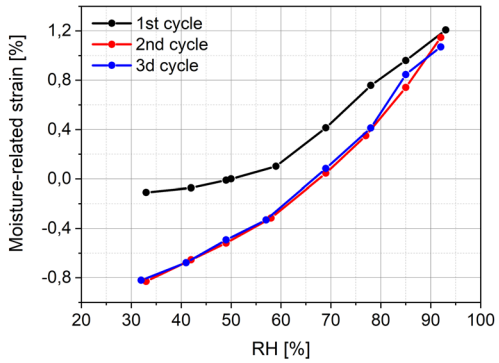

Fig. 7 Moisture-related strain of the CTS 1111 canvas liquid-sized with glue 63000 plotted as a function of RH

CTS 1111 canvas showed moisture-related expansion of 0.2% in the weft direction in the entire RH range and significant shrinkage of 0.5% in the warp direction at a high RH range. Glue sizing led to a considerable increase in swelling of the composite material in the less stiff warp direction, completely overriding the shrinkage of the untreated canvas. The approximate average moisture coefficients of dimensional change α_{RH} were determined by dividing the overall swelling from dry to wet conditions by the RH change in each direction (Table 6). The value of $3 \cdot 10^{-2}$% per 1% RH in the warp direction obtained for both of the glue-sized specimens was close to $4 \cdot 10^{-2}$% per 1% RH determined for the glue alone [21, 22]. In contrast, swelling of the glue-sized specimens in the stiffer weft direction was much smaller than for the glue alone, being clearly affected by the fabric.

Conclusions

The most general conclusion from this study is that glue-sized canvas is composite support in canvas paintings. Both the textile structure and material characteristics of the glue play significant roles in the composite performance. While preserving an anisotropy of mechanical properties which—as in the textile—depend on the relation of the direction of measurement to weft and warp, a sizing provided the composite material with high stiffness even at low loading corresponding to slack- and crimp removal regions in the untreated textile. In turn, a chalk-glue ground laid on the sized canvas formed a uniform layer exhibiting no differences in the load-extensions curves in the different weave directions up to the critical strain of approximately 0.002 corresponding to the elongation at break for grounds at the RH low- and mid-range.

The nominal moduli of elasticity of glue-sized canvases measured at a given RH and weave direction did not correlate reliably with the woven geometries of substrate canvases, the types of glue and the application procedures. The parameter showed high specimen-to-specimen variability reflected in high-standard deviations of individual sets of data and a low R-squared value derived from calculations of the best fit of relationships between the moduli of elasticity and RH. It was demonstrated that the reason for the observed variability lies in the inhomogeneity of glue application which needs to be considered as an inherent characteristic of the sized support canvas. As a result, the average, best-fit relationships between nominal moduli of elasticity and RH derived in this study are meaningful synthetic information which can be used in modelling canvas paintings as a physical system.

Swelling of glue sizing dominated the moisture-induced swelling of the composite material in the less stiff warp direction, completely overriding the shrinkage of the untreated canvas, whilst the dimensional change was smaller in the stiffer weft direction being clearly affected by the textile.

The observations modify and refine the current model of the assembly of the layers that constitute the painting subjected to high levels of RH. The demonstrated magnitude and anisotropy in the moisture-induced expansion of sized canvas on increasing RH inevitable causes deformations of canvas paintings. A correlation between the deformations and risk of physical damage to paint layers needs to be established by modelling and experimental work.

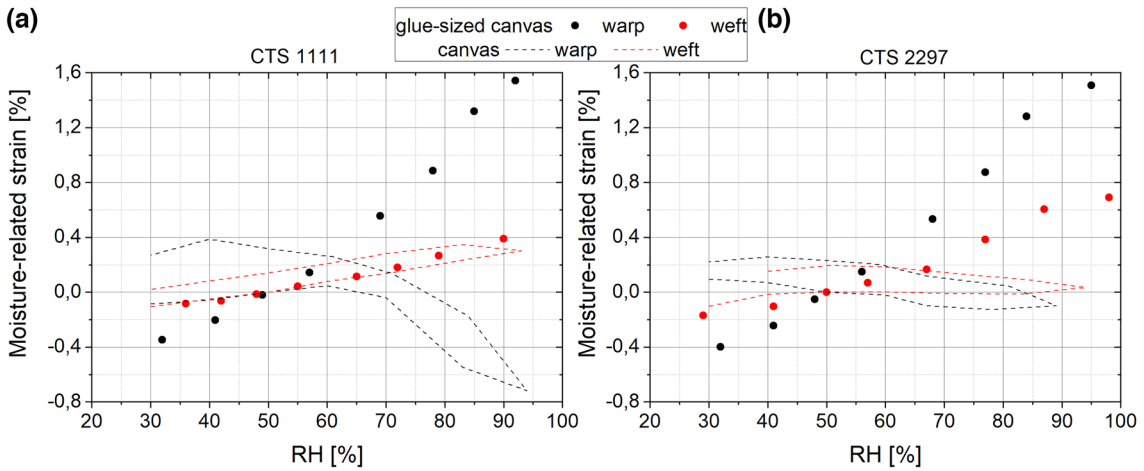

Fig. 8 Moisture-related dimensional changes of canvases: **a** CTS 1111; **b** CTS 2297, untreated and liquid-sized with glue 63000, plotted as a function of RH

Table 6 Moisture coefficients of dimensional change α_{RH} in two weave directions in the two glue-sized canvases analysed

Canvas	Weave direction	α_{RH} (10^{-2}%/% RH)
CTS 1111	Weft	0.9
	Warp	3.2
CTS 2297	Weft	1.2
	Warp	3.0

Abbreviations
PVC: Pigment volume concentration; RH: Relative humidity; w/w: Weight per weight.

Supplementary Information

The online version contains supplementary material available at https://doi.org/10.1186/s40494-022-00794-3.

Additional file 1. Nominal elasticity moduli of the materials investigated (in MPa).

Acknowledgements
Ana María Garcia-Castillo of the Institute of Information and Communication Technologies (ITACA) of the Universitat Politècnica de València is gratefully acknowledged for her involvement in the preparation of specimens.

Author contributions
LFL, CKA, MS, ŁB conceived the research hypotheses and the plan of experiments, AJ and ŁB developed the methodology, LFL prepared the specimens, AJ and KP performed the experimental work, AJ, RK, ŁB analysed and interpreted the results, RK wrote the first draft of the manuscript. All authors discussed the research outcome, as well as developed the manuscript. All authors read and approved the final manuscript.

Funding
This work was funded by the European Union's Horizon 2020 research and innovation program under grant agreement No. 814624 and the statutory research fund of the Jerzy Haber Institute of Catalysis and Surface Chemistry Polish Academy of Sciences. Łukasz Bratasz's work was financed by the Polish National Agency for Academic Exchange, project Polish Returns [Grant PPN/PPO/2018/1/00004/U/00001].

Availability of data and materials
All data needed to evaluate the conclusions in the paper are present in the paper and/or the Additional File. Additional data related to this paper may be requested from the corresponding author.

Declarations

Competing interests
The authors declare that they have no competing interests.

Author details
[1]Jerzy Haber Institute of Catalysis and Surface Chemistry Polish Academy of Sciences, 30-239 Kraków, Poland. [2]Universitat Politècnica de València, Instituto Universitario de Restauración del Patrimonio, 46022 Valencia, Spain. [3]The Royal Danish Academy, Conservation, Copenhagen, Denmark. [4]Universitat Politècnica de València, Instituto de Tecnologia de Materiales, 46022 Valencia, Spain.

Received: 22 June 2022 Accepted: 17 September 2022
Published online: 10 October 2022

References

1. Mecklenburg MF. Determining the acceptable ranges of RH and T in museums and galleries, Part 1. A report of the Museum Conservation Institute, the Smithsonian Institution. 2011. http://www.si.edu/mci/english/learn_more/publications/reports.html. Accessed 3 Jun 2022.
2. Karpowicz A. In-plane deformation of films of size on paintings in the glass transition region. Stud Conserv. 1989;34:67–74.
3. Krzemień L, Łukomski M, Bratasz Ł, Kozłowski R, Mecklenburg MF. Mechanism of craquelure pattern formation on panel paintings. Stud Conserv. 2016;61:324–30.
4. Mecklenburg MF. Some aspects of the mechanical behaviour of fabric supported paintings. A report to the Smithsonian Institution; 1982. In: Rogala DV, DePriest PT, Charola AE, Koestler RJ, editors. The mechanics of art materials and its future in heritage science, Smithsonian Contributions

to Museum Conservation, No. 10. Washington, D.C.: Smithsonian Scholarly Press; 2019. p. 107–30.
5. Hedley G. Relative humidity and the stress/strain response of canvas paintings: uniaxial measurements of naturally aged samples. Stud Conserv. 1988;33:133–48.
6. Bratasz Ł, Łukomski M, Klisińska-Kopacz A, Zawadzki W, Dzierżęga K, Bartosik M, Sobczyk J, Lennard FJ, Kozłowski R. Risk of climate-induced damage in historic textiles. Strain. 2015;51:78–88.
7. Andersen CK. Lined canvas paintings. Mechanical properties and structural response to fluctuating relative humidity, exemplified by the collection of Danish Golden Age paintings at Statens Museum for Kunst. Thesis. KADK Royal Danish Academy of Fine Arts; 2013.
8. Andersen CK, Mecklenburg MF, Scharff M, Wadum J. With the best intentions. Wax-resin lining of Danish Golden Age paintings (early 19th century) on canvas and changed response to RH. In: Bridgland J, editor. ICOM Committee for Conservation 14th triennial conference, Melbourne, 15–19 September 2014. Preprints 14.
9. Hendrickx R, Ferreira ESB, Boon JJ, Desmarais G, Derome D, Angelova L, Mannes D, Kaestner A, Huinink HP, Kuijpers CJ, Voogt B, Richardson E. Distribution of moisture in reconstructed oil paintings on canvas during absorption and drying: a neutron radiography and NMR study. Stud Conserv. 2017;62:393–409.
10. Hendrickx R, Desmarais G, Weder M, Ferreira ESB, Derome D. Moisture uptake and permeability of canvas paintings and their components. J Cult Herit. 2015;19:445–53.
11. Hedley GA. The effect of beeswax/resin impregnation on the tensile properties of canvas. In: ICOM Committee for Conservation 4th triennial meeting, Venice, 13–18 October 1975. Preprints 75/11/7. Paris: International Council of Museums; 1975.
12. Mehra VR. Minimizing strain and stress in lining canvas paintings. In: ICOM Committee for Conservation 6th triennial meeting, Ottawa, 21–25 September 1981. Preprints 81/2/14. Paris: International Council of Museums; 1981.
13. Young CRT, Hibberd RD. Biaxial tensile testing of paintings on canvas. Stud Conserv. 1999;44:129–41.
14. Penava Ž, Penava DŠ, Tkalec M. Experimental analysis of the tensile properties of painting canvas. Autex Res J. 2016;16:182–95.
15. Stols-Witlox M. A perfect ground. London: Archetype Publications; 2017. p. 50–5.
16. Erhardt D, Mecklenburg MF, Tumosa ChS. Long-term chemical and physical processes in oil paint films. Stud Conserv. 2005;50:143–50.
17. Fuster Lopez L. Estudio de la idondeidad de las masillas de relleno en el tratamiento de lagunas en pintura sobre lienzo. Thesis. Universidad Politecnica de Valencia; 2005.
18. Mecklenburg MF, Tumosa ChS. An introduction into the mechanical behavior of paintings under rapid loading conditions. In: Mecklenburg MF, editor. Art in transit: studies in the transport of paintings. Washington, D.C.: National Gallery of Art; 1991. p. 137–71.
19. Berger GA, Russell WH. Interaction between canvas and paint film in response to environmental changes. Stud Conserv. 1994;39:73–86.
20. Rachwał B, Bratasz Ł, Krzemień L, Łukomski M, Kozłowski R. Fatigue damage of the gesso layer in panel paintings subjected to changing climate conditions. Strain. 2012;48:474–81.
21. Bridarolli A, Freeman AA, Fujisawa N, Łukomski L. Mechanical properties of mammalian and fish glues over range of temperature and humidity. J Cult Herit. 2022;53:226–35.
22. Mecklenburg MF. Some mechanical and physical properties of gilding gesso. In: Bigelow D, Come E, Landrey GJ, van Horne C, editors. Gilded wood: conservation and history. Madison: Sound View Press; 1991. p. 163–70.

Publisher's Note